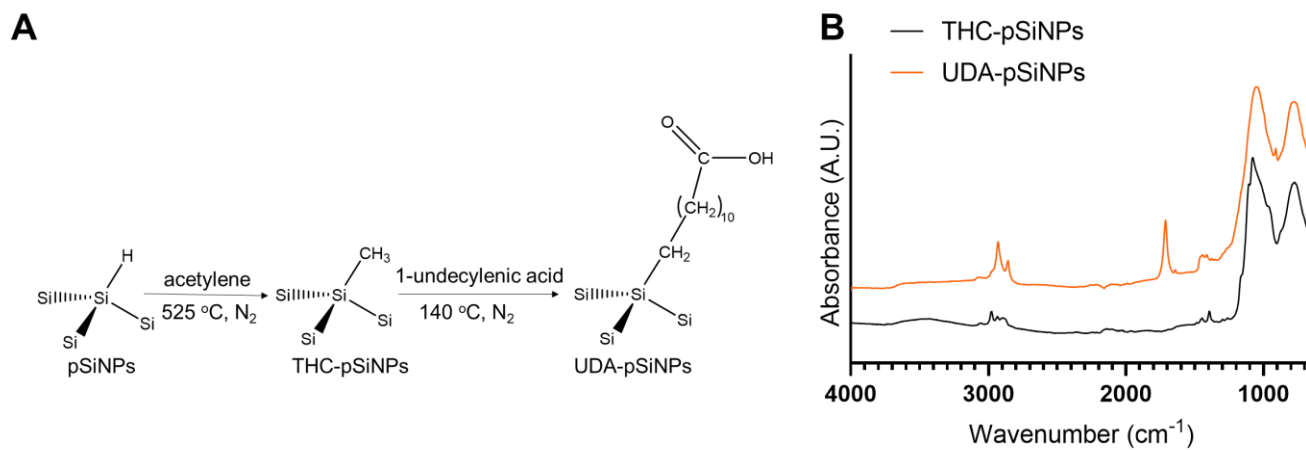
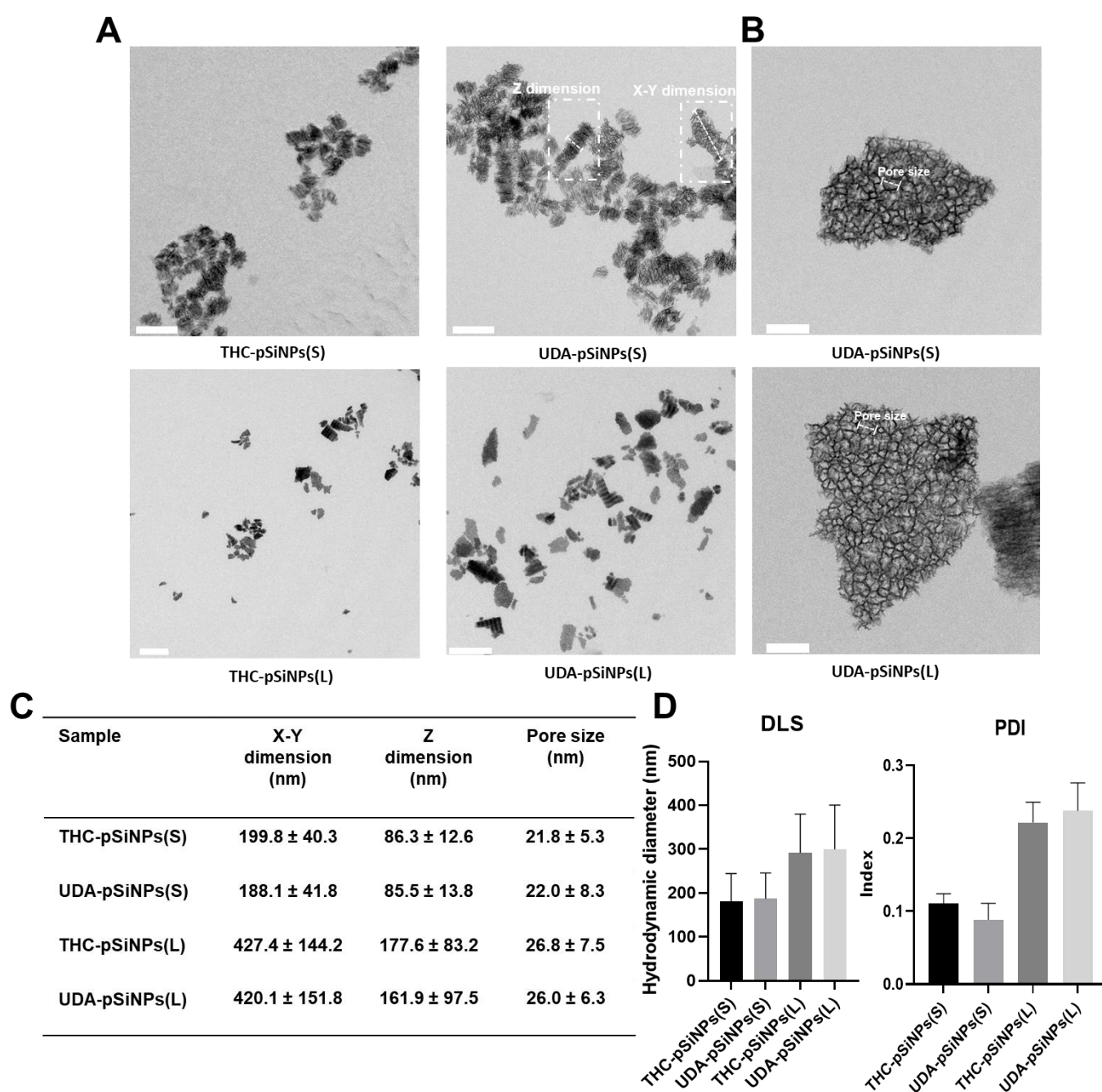


## Supplementary Materials



**Figure S1.** (A) Schematic synthesis of fabrication of UDA-pSiNPs from pSiNPs via acetylene and 1-undecylenic acid (B) ATR-FTIR spectra of THC-pSiNPs and the subsequent hydrosilylation with undecylenic acid (UDA-pSiNPs).



**Figure S2.** Characterization of THC-pSiNPs(S), UDA-pSiNPs(S), THC-pSiNPs(L) and UDA-pSiNPs(L). (A) Bright field transmission electron microscopy (BFTEM) images THC-pSiNPs(S), UDA-pSiNPs(S), THC-pSiNPs(L) and UDA-pSiNPs(L) in low magnification (Scale bar = 200 nm for small pSiNPs image and scale bar = 1000 nm for large pSiNPs image). (B) BFTEM images UDA-pSiNPs(S) and UDA-pSiNPs(L) in high magnification (Scale bar = 100 nm for both pSiNPs image). (C) Analysis of nanoparticles in their sizes in length (X-Y) and thickness (Z), and their pore size (the values are shown by mean ± sd, N=20) (D) The hydrodynamic diameter and polydispersity (PDI) of THC-pSiNPs(S), UDA-pSiNPs(S), THC-pSiNPs(L) and UDA-pSiNPs(L). Data are shown as mean ± sd, N = 3.

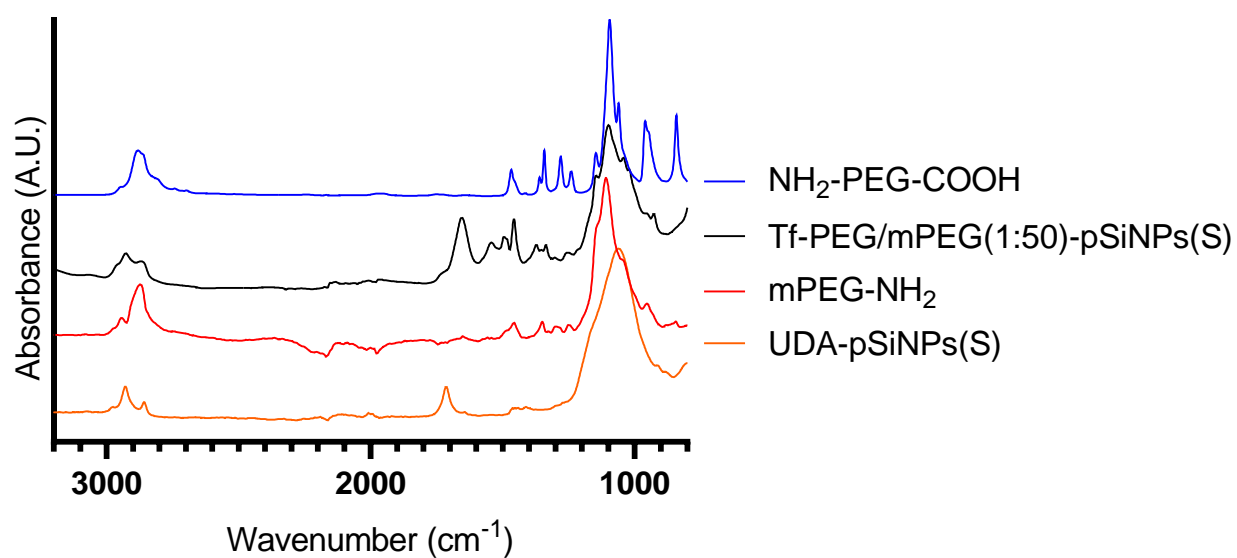
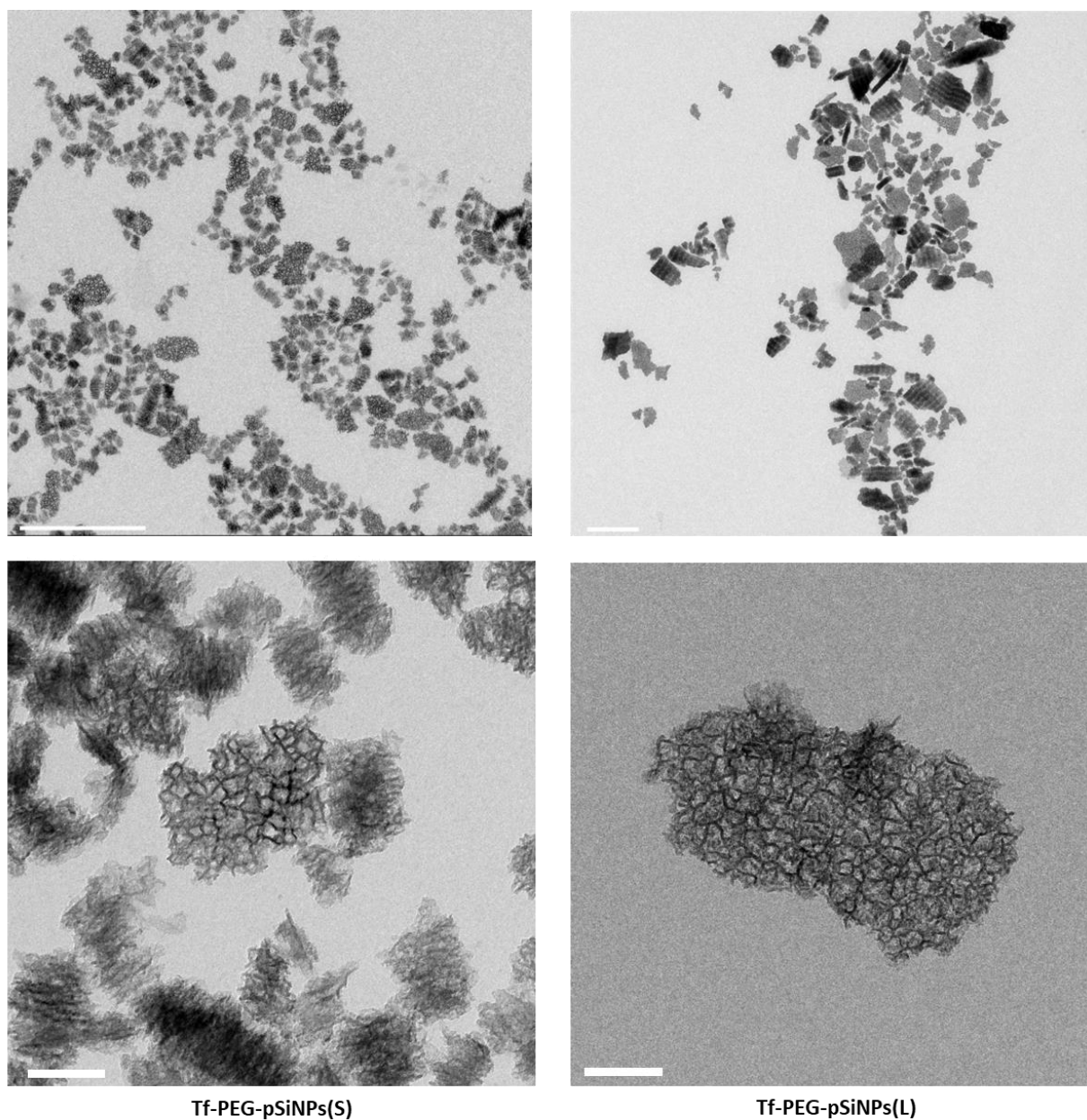


**Figure S3.** ATR-FTIR spectra of mPEG-NH<sub>2</sub> and NH<sub>2</sub>-PEG-COOH in comparison with UDA-pSiNPs(S) and Tf-PEG/mPEG(1:50)-pSiNPs(S).



Tf-PEG-pSiNPs(S)		Tf-PEG-pSiNPs(L)	
Sample	X-Y dimension (nm)	Z dimension (nm)	Pore size (nm)
Tf-PEG-pSiNPs(S)	$203.5 \pm 41.6$	$86.4 \pm 14.2$	$25.7 \pm 7.3$
Tf-PEG-pSiNPs(L)	$424.3 \pm 131.4$	$172.2 \pm 117.5$	$24.1 \pm 4.5$

**Figure S4.** BFTEM images Tf-PEG-pSiNPs(S) and Tf-PEG-pSiNPs(L) in low(top) and high (bottom) magnification and their length (x-y dimension), thickness (z-dimension), and pore size (values are shown by mean  $\pm$  sd, N=80, Scale bar = 1000 nm in low magnification images, Scale bar = 100 nm in high magnification images).

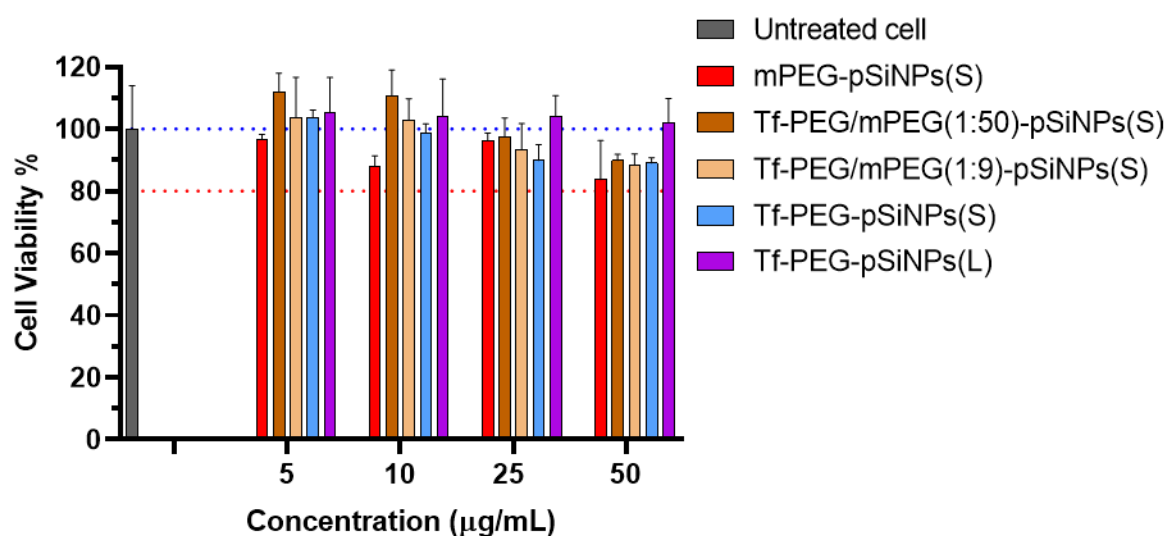


**Figure S5.** Cell viability results for hCMEC/D3 cells treated with different concentrations (5, 10, 25, 50 µg/mL) of modified pSiNPs for 48 h. Control (untreated hCMEC/D3 cells) was included. The values are shown by mean  $\pm$  sd, N = 3.

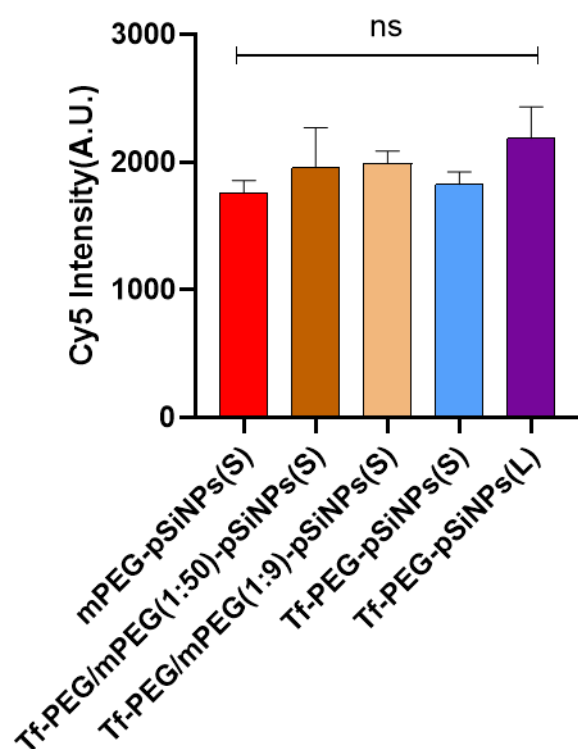


**Figure S6.** Cy5 intensity of all modified pSiNPs on a per mass basis. All samples maintained similar Cy5 intensity without significant differences. The values are shown by mean  $\pm$  sd, N=3, One-way ANOVA test.

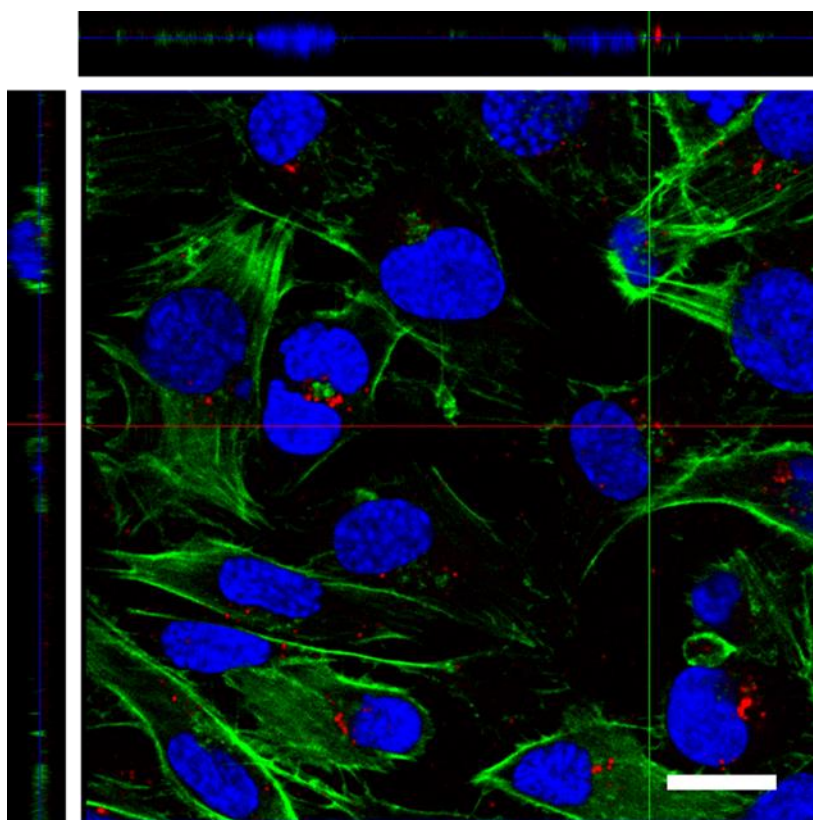


**Figure S7.** Cellular uptake of Tf-PEG-pSiNPs(S) in hCMEC/D3 with z-stack scan. (blue = nucleus, green = F-actin, red = nanoparticles, scale bar = 20  $\mu\text{m}$ ). The nanoparticle concentration was 5  $\mu\text{g/mL}$ .



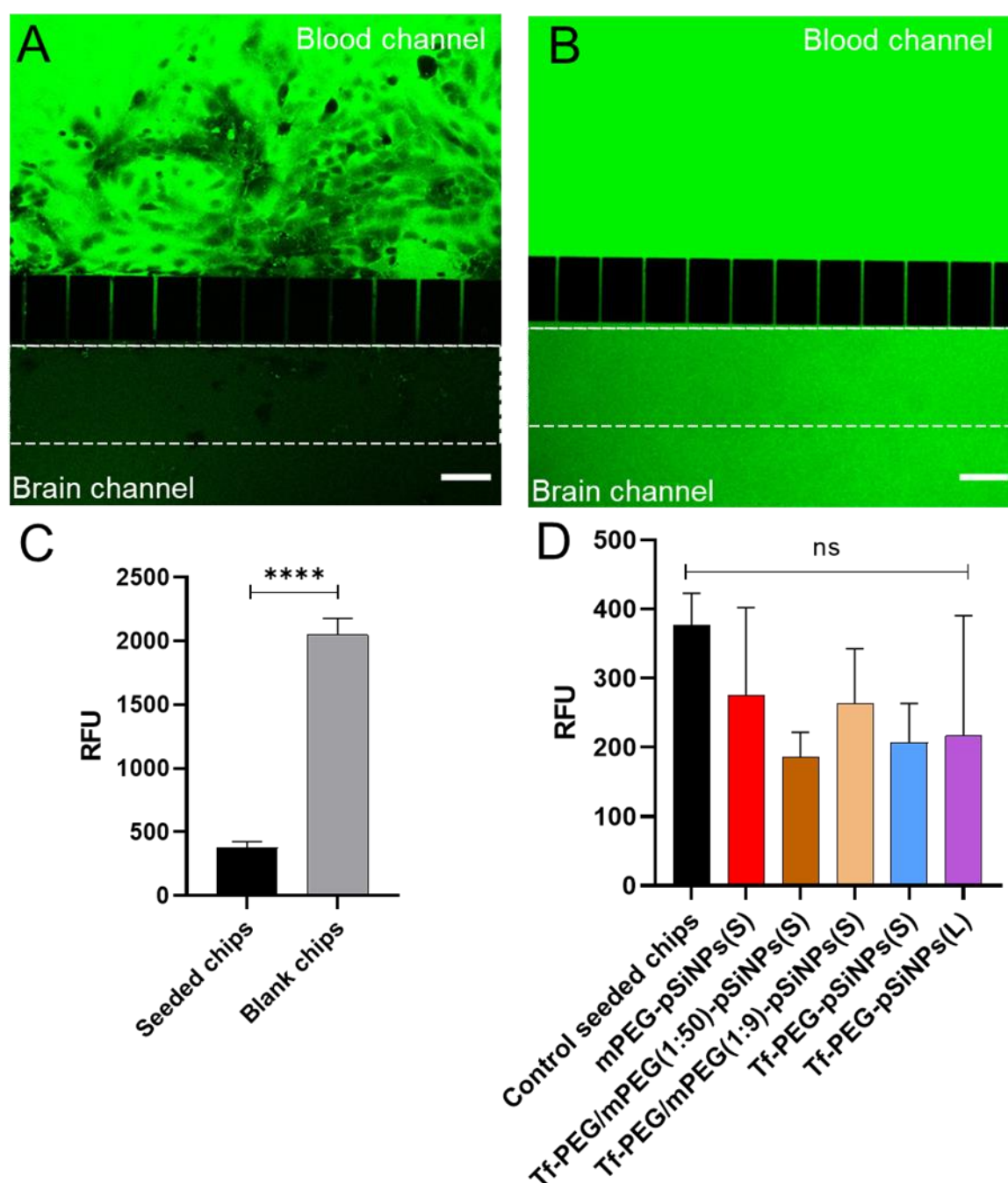


**Figure S8.** Validation of BBB-on-a-chip model. Comparison of FITC-dextran (10 kDa, 25  $\mu\text{g/mL}$ ) permeation into brain channels in (A) hCMEC/D3 seeded chips and (B) in blank control chips; scale bar: 50  $\mu\text{m}$ . FITC-dextran largely remained in the blood channel in cultured chips while it was freely distributed in both channels in blank control chips. (C) Corresponding relative fluorescence intensity (RFU) of FITC-dextran in brain channels in cultured and control chips. RFU of brain channels in cultured chips was significantly lower than in control chips. The values are shown by mean  $\pm$  sd,  $N = 3$ , Student's t-test,  $P^{****} < 0.0001$ . (D) RFU of FITC-dextran in brain channel in all tested NPs cultured chips showed no significant difference to control seeded chips. The values are shown by mean  $\pm$  sd,  $N > 3$ , One-way ANOVA test.

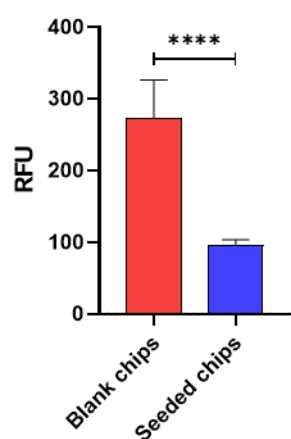


**Figure S9.** Transportation of Tf-pSiNPs from blood to brain channels after flowing for 4 h. Corresponding RFU of pSiNPs crossing blood channels in blank chips and hCMEC/D3 seeded chips. The values are shown by mean  $\pm$  sd, N = 3, Student's t-test, P\*\*\*\* < 0.0001.